

Received October 24, 2019, accepted November 13, 2019, date of publication November 18, 2019, date of current version November 27, 2019.

Digital Object Identifier 10.1109/ACCESS.2019.2953997

# A Finite-Time Robust Adaptive Sliding Mode Control for Electro-Optical Targeting System With Friction Compensation

XINLI ZHOU  AND XINGFEI LI 

The State Key Laboratory of Precision Measuring Technology and Instruments, Tianjin University, Tianjin 300072, China

Corresponding author: Xingfei Li (lix\_f\_tju@163.com)

This work was supported in part by the Foundation of National Natural Science Foundation of China under Grant 61427810 and Grant 61733012.

**ABSTRACT** In this paper, a novel finite-time robust adaptive nonsingular fast terminal sliding mode control strategy is designed to achieve high performance control for an electro-optical targeting system which is subjected to nonlinear friction and disturbance torque. First, a robust adaptive control technique is constructed to compensate modified LuGre model and disturbance torque. Then, a nonsingular terminal fast sliding mode is integrated into the robust adaptive control technique to implement response rapidity and enhance the robustness of the closed-loop system. Furthermore, the control strategy is proved by Lyapunov criterion within finite time. Finally, simulation and experimental results indicate that high accuracy, fast response and stable control performance are obtained by the proposed control strategy for the electro-optical targeting system.


**INDEX TERMS** Electro-optical targeting system, robust adaptive control, nonsingular fast terminal sliding mode control, friction, finite-time.

## I. INTRODUCTION

Electro-optical targeting system has raised considerable attention and played a more and more important roles recently in various realms, from ships, land, aircraft to satellites, civilian to military [1], [2]. Due to the increasingly harsh application environment and complexity of electro-optical targeting system, designing a high-performance control strategy is of significant importance, also remains a key technique for electro-optical targeting system. However, nonlinear friction and the disturbance torque causing by uncertainties, model variation, coupling effect between rotating gimbal axes and external disturbance [3], lead to strong nonlinearity for electro-optical targeting system and make it difficult to realize high precise motion. Particularly, when ultra long distance monitoring and tracking target, the visible light camera or infrared camera of electro-optical targeting system is at its longest focus state, meanwhile its angle field of view is extremely small. Consequently, the strong nonlinearity could easily decrease the control accuracy and degrade the

performance of remotely monitoring and tracking in manual or automatic mode, even result in image smear or target loss from field of view. Moreover, the friction, which is the most significant nonlinear factor among other nonlinearities, inevitably affects the performance of control motion, even causes the overall system instability [4]. Therefore, in order to tackle above problems, designing a high-performance control strategy for electro-optical targeting system remains a challenging task.

The study on friction compensation has become one of the hotspots in recent decades and many researchers have been involved in it. Adaptive control strategy is deemed as a effective method for servo system with respect to nonlinear phenomenon. In [5], an adaptive backstepping control strategy was proposed to decrease the adverse effect of friction under different motional conditions and realize a good servo control precision. An adaptive controller along with fast convergence sliding mode reaching law was presented to deal with nonlinear friction, and improve the tracking accuracy for a two-axle voice coil linear motor gantry in [6]. In [7], an adaptive backstepping control strategy based on a novel modified LuGre friction model with continuous property was

The associate editor coordinating the review of this manuscript and approving it for publication was Ning Sun .

designed to tackle nonlinear friction as well as uncertain parameters for hydraulic system. In order to handle external disturbances problems, a robust control along with efficient speed control were presented to improve the performance of three phase induction motor [8]. In [9], a backstepping nonlinear controller combining with a speed observer was proposed for induction motor to implement speed control without sensors. A hybrid control strategy that backstepping technique, adaptive control and  $H_\infty$  control are combined to improve the robust of servo system [10]. In [11], a RISE feedback along with continuous adaptive robust algorithm were presented to tackle with model uncertain in nonlinear closed-loop systems. To a certain extent, the above control strategies lack the capability to implement high accurate dynamic control, owing to nonlinear friction, model variation and external disturbance, or one of them.

Sliding mode control (SMC) method is deemed as a effective control strategy which has many advantages including strong robustness to parametric variation, controllable convergence rate, and excellent anti-disturbance ability facing with friction and disturbance torque. A compound control method was designed by sliding mode control with backstepping method to deal with negative impedance feature for constant power load [12]. In [13], an adaptive sliding mode controller which is depended on model was adopted to achieve a high accurate control for a boiler-turbine system. A sliding mode controller with filters and sliding mode observers was designed to improve the performance of inertia wheel pendulum [14]. In [15], a sliding mode control method which based on a new synchronization control law along with Nussbaum gain technique was presented to deal with system time synchronization problem for chaotic centrifugal flywheel governor. An novel adaptive sliding mode approach was developed to reducing chattering phenomenon as well as nonlinear disturbances for nonlinear MIMO system [16]. In [17], a hybrid control strategy which combines a sliding mode control with a variable gain and time-delay controller to implement a robust characteristic for robot manipulator. Although these algorithms have been thoroughly researched and implemented in various applications, majority of them guarantees asymptotic tracking performance, without focusing on the performance of convergence speed and finite time response.

Thus, a closed-loop system with the feature of finite time convergence and stabilisation was proposed by using terminal SMC [18]. In [19], a terminal SMC makes it possible for closed-loop system to have anti-disturbance capacity under the condition of external disturbance and converge tracking error rapidly to zero in finite time. Inevitably, terminal SMC is subjected to a singularity phenomenon [20]. Then, nonsingular terminal sliding mode (NTSM) approach which needs no extra procedures was proposed to tackle with the singularity phenomenon [21], [22]. In [23], a nonsingular terminal fast sliding mode (NFTSM) control method which has a more rapidly convergence rate compared to NTSM was presented to curb the singular problem. In [24], a finite-time

robust stabilized sliding mode control with nonsingular terminal sliding surface was adopted to solve the matched uncertainties problem for second order nonlinear plants. In [25], a fast reaching law which was integrating into a sliding mode controller to speed up the the reaching rate, was superior to conventional reaching law. A nonsingular terminal sliding mode strategy was presented to achieve a high accurate position tracking control for linear piezoelectric ceramic actuators which are suffered from nonlinear friction, parametric variation and disturbances [26]. However, it is still of a difficult but challenging work to design a high-performance control strategy for electro-optical targeting system owing to friction and disturbance torque, which is not yet thoroughly solved.

In this paper, a novel combination of NFTSM with adaptive robust control for electro-optical targeting system is proposed. A robust adaptive control technique is proposed to handle with nonlinear friction and disturbance torque via estimating the unmeasurable and variable parameters from the established nonlinear system model. Then, a nonsingular terminal fast sliding mode is integrated into the robust adaptive control technique to guarantee response rapidity and enhance the robustness of the nonlinear system. The method is proved within finite time by utilizing Lyapunov theory. Finally, experimental results under different conditions, including step test, low frequency test and multiple frequency test, demonstrate that the designed controller is excellent and well suitable for electro-optical targeting system. The contributions of this paper are summarized as follows:

- 1 A robust adaptive control technique is proposed to handle with nonlinear friction and disturbance torque via estimating the unmeasurable and variable parameters from disturbance torque and modified LuGre model.
- 2 A nonsingular terminal fast sliding mode are integrated into the robust adaptive control technique to guarantee response rapidity and enhance the robustness of the nonlinear system. The method is proved within finite time by utilizing Lyapunov theory.
- 3 Experimental results under different conditions, including step test, single frequency sinusoidal test and multiple frequency sinusoidal test, demonstrate that the designed controller in this paper is superior to the method in [3].

## II. PROBLEM STATEMENT AND PRELIMINARIES

The main function of electro-optical targeting system (EOTS) includes real-time monitoring, tracking and recording. The EOTS is able to cooperate with PC and other external devices such synthetic aperture radar (SAR), remote control weapon station and so on. When PC and other external devices send commands which can be deemed as reference signals to EOTS via serial interface or network interface, the EOTS tracks the reference signals accurately and rapidly. However, the friction and disturbance torque greatly decrease the control accuracy of pointing angle in such cases. Especially when ultra long distance monitoring target, the visible light

camera or infrared camera of electro-optical targeting system is at its longest focus state, meanwhile its angle field of view is extremely small. The friction as well as disturbance torque could easily degrade the performance of long distance monitoring and inspecting or even result in image smear and target loss from field of view. The working principle and the control flow charts of EOTS are presented in Fig.1 and Fig.2, respectively.

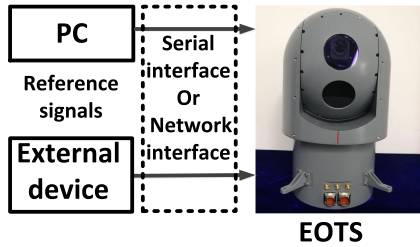


FIGURE 1. Working principle of EOTS.

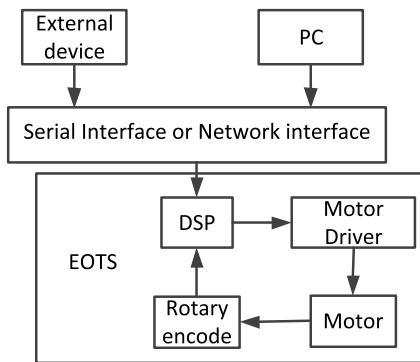


FIGURE 2. The control flow charts of EOTS.

**A. SYSTEM MATHEMATICAL MODEL**

Assumption 1: (1)Motor inductance is neglected. (2)The gimbal with payload is considered rigid. Then the mathematical system model [27] can be described as follows:

$$\begin{aligned}
 \dot{\theta} &= \omega \\
 J\dot{\omega} &= T_m - F_f - \Delta \\
 T_m &= K_t i_m \\
 i_m &= \frac{U - k_e \omega}{R}
 \end{aligned} \tag{1}$$

where  $J$  denotes the moment of inertia of gimbal with payload including visible light camera and infrared camera,  $\theta$  and  $\omega$  represent angle and angle rate.  $U$  is the digital control input.  $K_t$  and  $K_e$  indicate motor torque coefficient and motor back-EMF coefficient, respectively.  $R$  denotes motor resistance.  $F_m$  represents the motor torque output which is proportional to armature current  $i_m$ . While  $F_f$  denotes nonlinear friction force,  $\Delta$  indicates disturbance torque, including uncertainties, model variation, coupling effect between rotating gimbal axes and external disturbance.

**B. MODIFIED DYNAMIC LuGre MODEL**

Although several friction models have been analysed in recent works [28], [29]. In the following analysis, the friction model  $F_f$  has been selected as LuGre model [30], in which strobek effect, hysteresis, and so on are included.

$$F_f = \sigma_0 z + \sigma_1 \dot{z} + \sigma_2 \omega \tag{2}$$

$$\dot{z} = \omega - \frac{|\omega|}{g(\omega)} z \tag{3}$$

$$\sigma_0 g(\omega) = F_c + (F_s - F_c) e^{-\left(\frac{\omega}{\omega_s}\right)^2} \tag{4}$$

Here  $z$  represents the average deflection of bristles. The function  $g(\omega)$  is positive and known, depicting various friction effect such as strobek effect.  $\sigma_0$  represents the stiffness coefficient, and  $\sigma_1$  is the viscous friction coefficient.  $F_s$  and  $F_c$  denote static friction force and coulomb friction force, respectively.  $\omega(s)$  corresponds to the strobek angle rate.

The friction parameters will vary in the present of internal mass unbalance, nonuniform cutting surface and external environment perturbations, thus the adaptive parameters  $\mu, \nu$  are adopted to modified the standard LuGre model with fixed parameters. The modified LuGre model can be expressed as below

$$F_f = \mu(\sigma_0 z + \sigma_1 \dot{z}) + \nu \sigma_2 \omega \tag{5}$$

where  $\mu$  denotes the parametric variation for bristles average deflection,  $\nu$  represents the parametric perturbation in viscous friction. Moreover, they satisfy the bounded condition  $0 \leq \mu_{min} \leq \mu < \mu_{max}$  and  $0 \leq \nu_{min} \leq \nu \leq \nu_{max}$ .

Choosing  $\theta = x_1$  and  $\dot{\theta} = \omega = x_2$ , the overall mathematical system model can be written as the following form:

$$\begin{aligned}
 \dot{x}_1 &= x_2 \\
 \dot{x}_2 &= \frac{K_t}{JR} U - \frac{K_t K_e}{JR} \omega - \frac{1}{J} \mu z (\sigma_0 - \sigma_1 \frac{|\omega|}{g(\omega)}) \\
 &\quad - \frac{1}{J} (\mu \sigma_1 + \nu \sigma_2) \omega - \frac{\Delta}{J} \\
 y &= x_1
 \end{aligned} \tag{6}$$

**C. FRICTION MODEL PARAMETER IDENTIFICATION**

LuGre model has many attracted advantages for its simple mathematical form, easy real-time implementation and precise reflecting friction features. And its parameter identification [31] is composed of two fundamental parts, i.e., static and dynamic parameter identification. In the procedure of parameters identification, four static parameters and two dynamic parameters are estimated, respectively.

**1) STATIC PARAMETER IDENTIFICATION**

Set  $dz/dt = 0$ . Inserting equation (3)(4) into equation (2) yields the steady state motion:

$$F_f = (F_c + (F_s - F_c) e^{-\left(\frac{\omega}{\omega_s}\right)^2}) \text{sgn}(\omega) + \sigma_2 \omega = T_m \tag{7}$$

According to strobek curve, four static parameters could be obtained. Assumed that pitch axis stays stationary, the azimuth axis rotates with a series of incremental angle rate

values  $\{\omega_j\}_{j=1}^N$ , and corresponding values of digital control output are  $\{F_{mj}\}_{j=1}^N$ . Thus, the parameters vector is expressed as follows

$$X_s = [\hat{F}_c, \hat{T}_s, \hat{\omega}_s, \hat{\sigma}_2] \quad (8)$$

Define the identification error as

$$e(X_s, \omega_j) = T_{mj} - F_f(X_s, \omega_j) \quad (9)$$

where  $F_f(X_s, \omega_j)$  denotes desired friction. Taking the error objective function as follows:

$$I_x = \frac{1}{2} \sum_{j=1}^N e^2(X_s, \omega_j) \quad (10)$$

Finally, by minimizing the error objective function  $I_x$ , the four static parameters  $F_c, F_s, \omega_s$  and  $\sigma_2$  are obtained.

### 2) DYNAMIC PARAMETER IDENTIFICATION

The dynamic parameters  $\sigma_0$  and  $\sigma_1$  are obtained via presliding displacement method shown as follows:

$$\sigma'_0 \approx \frac{\Delta T}{\Delta \theta} \quad (11)$$

$$\sigma'_1 \approx 2\sqrt{\sigma'_0 M} - \sigma_2 \quad (12)$$

where  $M$  is the mass of the gimbal with payload including visible light camera and infrared camera.  $\Delta T$  and  $\Delta \theta$  are increment value of control torque and angle with same time interval. The least square method is introduced to identify the dynamic parameters  $\sigma_0$  and  $\sigma_1$ . Suppose that the vector in which parameters are to be identified, is shown as below

$$X_d = [\hat{\sigma}_0, \hat{\sigma}_1] \quad (13)$$

Define the identification error as

$$e(X_d, t_j) = \theta(t_j) - \theta(X_d, t_j) \quad (14)$$

where  $\theta(t_j)$  and  $\theta(X_d, t_j)$  are the angle from absolute magnetic rotary encoder and the angle from system mathematical model respectively, corresponding to moment  $t_j$ . Then the objective function is adopted as follows:

$$I_y = c_1 \sum_{j=1}^N e^2(X_s, \omega_j) + c_2 \max\{e(X_s, \omega_j)\} \quad (15)$$

Here,  $c_1$  and  $c_2$  represent weight coefficients. Thus, by making the objective function  $I_y$  minimized, the two dynamic parameters  $\sigma_0$  as well as  $\sigma_1$  can be precisely obtained.

### III. FINITE-TIME ROBUST ADAPTIVE NONSINGULAR FAST TERMINAL SLIDING MODE CONTROLLER

In this section, in order to decrease the tracking error, enhance the robustness and ensure response rapidity in the present of friction and disturbance torque, a finite-time robust adaptive NFTSM control strategy is proposed.

*Lemma 1:* (reaching time) [32]: Take into account nonlinear system  $\dot{x}_b = f(x_b(t))$ ,  $f(0) = 0$  and  $x_b(t) \in R^n$ .

Assumed that a positive defined scalar function  $V_b(x_b(t))$  is existing as below

$$\dot{V}_b(x_b(t)) \leq -\tau_1 V_b(x_b(t)) - \tau_2 V_b(x_b(t))^\theta \quad (16)$$

where  $\tau_1 > 0$ ,  $\tau_2 > 0$  and  $0 < \theta < 1$ , then the nonlinear system is stable within finite time. Moreover, the setting time  $T_1$  is gained as below:

$$T_1 \leq \frac{1}{\tau_1(1-\theta)} \ln \frac{\tau_1 V_b^{1-\theta}(x_b(t_0)) + \tau_2}{\tau_2} \quad (17)$$

where  $V_b(x_b(t_0))$  is the initial value of  $V_b(x_b(t))$ .

*Lemma 2:* (sliding time) [33]: Assume that a kind of nonsingular fast terminal sliding surface is expressed as below:

$$s(t) = \varepsilon(t) + k'_1 \text{sign}^{\psi_1}(\varepsilon(t)) + k'_2 \text{sign}^{\psi_2}(\dot{\varepsilon}(t)) \quad (18)$$

where  $k'_1, k'_2$  are positive constants,  $1 < \psi_2 < 2$  and  $\psi_1 > \psi_2$ . When  $s(t) = 0$ , the convergence time  $T_2$  of  $\varepsilon(t)$  is obtained as follows:

$$\begin{aligned} T_2 &= \int_0^{\varepsilon(0)} \frac{k_2'^{1/\psi_2'}}{(\varepsilon(t) + k_1'\varepsilon(t)^{\psi_1})^{1/\psi_2}} dx \\ &= \frac{\psi_2 |x(0)|^{1-1/\psi_2}}{k_1'(\psi_2 - 1)} \\ &\quad \cdot F\left(\frac{1}{\psi_2}, \frac{\psi_2 - 1}{(\psi_1 - 1)\psi_2}; 1 + \frac{\psi_2 - 1}{(\psi_1 - 1)\psi_2}; -k_1'|x(0)|^{\psi_1-1}\right) \end{aligned} \quad (19)$$

where  $\varepsilon(0)$  denotes the initial value of  $\varepsilon(t)$ ,  $F(\cdot)$  represents the Gaussian hypergeometric function shown as below. And the conditions of  $k'_1, k'_2, \psi_1, \psi_2$  indicate that  $F(\cdot)$  will ensure convergent. As usual, the exact form of  $F(\cdot)$  changes while the involved parameters varies. One can refer to the work [34] for Gauss hypergeometric function more thoroughly.

$$F(m, p; k; l) = \sum_{n=0}^{\infty} \frac{(m)_n (p)_n}{(k)_n n!} l^n$$

Assume that  $y_d$  is the reference signal, the angle tracking error is  $e_1 = y - y_d$ . Then its derivative term and two order derivative term are  $e_2 = \dot{y} - \dot{y}_d$  and  $\dot{e}_2 = \ddot{y} - \ddot{y}_d$ , respectively. Thus, the error dynamic of the closed-loop system can be expressed as

$$\begin{aligned} \dot{e}_1 &= e_2 \\ \dot{e}_2 &= \ddot{y}_d - \frac{K_t}{JR} U + \frac{K_1 K_e}{JR} \omega + \frac{1}{J} \mu z (\sigma_0 - \sigma_1 \frac{|\omega|}{g(\omega)}) \\ &\quad + \frac{1}{J} (\mu \sigma_1 + \nu \sigma_2) \omega + \frac{\Delta}{J} \end{aligned} \quad (20)$$

*Assumption 2:* The reference output  $y_r(t)$  is a twice differentiable continuous function in terms of  $t$ .

*Assumption 3:* The disturbance torque  $\Delta$ , including uncertainties, model variation, coupling effect between rotating gimbal axes and external disturbance, are usually unmeasurable and assume to be bounded owing to a positive function

as follows  $|\Delta| \leq \delta$ , where  $\delta$  denotes the upper bound of the lumped uncertainty.

Because the state  $z$  in LuGre friction model is unmeasurable, a friction observer is designed to estimate the state  $z$ . The method of the friction observer is first proposed in [30], then many scholars have adopted this method owing to its effectiveness and practicability. In this paper, a nonlinear friction observer is adopted to tackle the unmeasured friction displacement state  $z$ . Supposing the estimated value of observer defines as  $\hat{z}$ , the relationship between nonlinear friction observer  $\hat{z}$  and its differential term  $\dot{\hat{z}}$  are express as follows

$$\dot{\hat{z}} = \omega - \frac{|\omega|}{g(\omega)}\hat{z} + l_0 \tag{21}$$

where  $l_0$  in the observer is dynamic terms yet to be obtained. The error of friction observer  $\tilde{z}$  is written as follows

$$\tilde{z} = z - \hat{z} \tag{22}$$

The derivative of  $\tilde{z}$  is expressed as below

$$\dot{\tilde{z}} = -\frac{|\omega|}{g(\omega)}\tilde{z} - l_0 \tag{23}$$

From above discussions, an NFTSM surface  $s(t)$  which can strengthen the robustness, improve control accuracy as well as rapidity and avoid nonsingular problem is introduced as follows:

$$s(t) = e_1 + k_1 \text{sign}^{\phi_1}(e_1) + k_2 \text{sign}^{\phi_2}(e_2) \tag{24}$$

where  $k_1, k_2$  are positive constants,  $1 < \phi_2 < 2$  and  $\phi_1 > \phi_2$ .

*Remark 1:* Note that the system state converges to  $e_1 = 0$  in finite time for any given initial condition  $e_1(0) \neq 0$ . In one case, when the system state is far from the equilibrium state initially, the equation (24) is approximated to the follows equation

$$s(t) = e_1 + k_1 \text{sign}^{\phi_1}(e_1) \tag{25}$$

where the subitem  $k_1 \text{sign}^{\phi_1}(e_1)$  which ensures a fast convergence rate dominates the most compared to  $k_2 \text{sign}^{\phi_2}(e_2)$ . In another case, when the system is close to the equilibrium state, then equation (24) is simplified approximately as follows

$$s(t) = e_1 + k_2 \text{sign}^{\phi_2}(e_2) \tag{26}$$

where the subitem  $k_2 \text{sign}^{\phi_2}(e_2)$  guarantees the system convergence in finite time.

Considering the closed-loop system, the following reaching law is selected as:

$$\dot{s}(t) = -k_3 \text{sign}(s(t)) - k_4 s(t) \tag{27}$$

where  $k_3 > 0, k_4 > 0$ . Then sliding mode reaching condition is expressed as follows:

$$s\dot{s} = -k_3 s - k_4 s^2 \leq -k_3 |s| \leq 0 \tag{28}$$

To obtain satisfactory tracking angle, the controller  $U(t)$  is designed containing two parts  $U_{equation}(t)$  and  $U_{sw}(t)$ :

$$U(t) = U_{equation}(t) + U_{sw}(t) \tag{29}$$

$$\begin{aligned} U_{equation}(t) = & \frac{JR}{k_t}(\ddot{y}_d + \frac{k_1 k_e}{JR}\omega + \frac{1}{J}\mu z(\sigma_0 - \sigma_1 \frac{|\omega|}{g(\omega)})) \\ & + \frac{1}{J}(\mu\sigma_1 + \nu\sigma_2)\omega + \frac{\Delta}{J} \\ & + \frac{1}{k_2\phi_2} \text{sign}^{2-\phi_2} e_2 (1 + k_1\phi_1 \text{sign}^{\phi_1-1} e_1) \end{aligned} \tag{30}$$

$$U_{sw}(t) = \frac{JR}{k_t}(k_3 \text{sign}(s) + k_4 s) \tag{31}$$

Note that the control strategy (29)-(31) cannot be guaranteed in practical application owing to the unknown parameters  $\mu$  and  $\nu$ , the unmeasurable friction state  $z$  and the unmeasurable varying parameters  $\Delta$ . Thus, it is essential to adopt the adaptive term to estimate the above unknown or unmeasurable parameters.

$$U(t) = \bar{U}_{equation}(t) + U_{sw}(t) \tag{32}$$

$$\begin{aligned} \bar{U}_{equation}(t) = & \frac{JR}{k_t}(\ddot{y}_d + \frac{k_1 k_e}{JR}\omega + \frac{1}{J}\hat{\mu}\hat{z}(\sigma_0 - \sigma_1 \frac{|\omega|}{g(\omega)})) \\ & + \frac{1}{J}(\hat{\mu}\sigma_1 + \hat{\nu}\sigma_2)\omega + \frac{\hat{\Delta}}{J} \\ & + \frac{1}{k_2\phi_2} \text{sign}^{2-\phi_2} e_2 (1 + k_1\phi_1 \text{sign}^{\phi_1-1} e_1) \end{aligned} \tag{33}$$

$$U_{sw}(t) = \frac{JR}{k_t}(k_3 \text{sign}(s) + k_4 s) \tag{34}$$

$\hat{\Delta}$  denotes the estimate value of parameter  $\Delta$ , and the friction state  $z$  is estimated by  $\hat{z}$ .

*Remark 2:* The first term of equivalent control law  $U_{equation}(t)$  has capability to guarantees fast convergence within finite time no matter where the system states are, far from or close to the sliding surface. Meanwhile, the second term  $U_{sw}(t)$  is designed to be more robust for the system in the present of external perturbations and parametric uncertainties.

By substituting equation (32) into equation (20) the error dynamic of the system can be rewritten as

$$\begin{aligned} \dot{e}_1 = & e_2 \\ \dot{e}_2 = & \frac{1}{J}(\mu z - \hat{\mu}\hat{z})(\sigma_0 - \sigma_1 \frac{|\omega|}{g(\omega)}) + \frac{1}{J}(\mu - \hat{\mu})\sigma_1 \omega \\ & + \frac{1}{J}(\nu - \hat{\nu})\sigma_2 \omega + \frac{1}{J}(\Delta - \hat{\Delta}) \\ & - \frac{1}{k_2\phi_2} \text{sign}^{2-\phi_2} e_2 (1 + k_1\phi_1 \text{sign}^{\phi_1-1} e) \\ & - k_3 \text{sign}(s) - k_4 s \end{aligned} \tag{35}$$

*Theorem 1:* Consider the closed-loop system (20) with the NFTSM surface defined in (24). With the following

control law:

$$\begin{aligned}
 U(t) = & \frac{JR}{k_t}(\ddot{y}_d + \frac{k_1 k_e}{JR}\omega + \frac{1}{J}\hat{\mu}\hat{z}(\sigma_0 - \sigma_1 \frac{|\omega|}{g(\omega)})) \\
 & + \frac{1}{J}(\hat{\mu}\sigma_1 + \hat{v}\sigma_2)\omega + \frac{\hat{\Delta}}{J} \\
 & + \frac{1}{k_2\phi_2} \text{sign}^{2-\phi_2} e_2 (1 + k_1\phi_1 \text{sign}^{\phi_1-1} e_1) \\
 & + \frac{JR}{k_t}(k_3 \text{sign}(s) + k_4 s) \tag{36}
 \end{aligned}$$

and the friction observer

$$\dot{\hat{z}} = -\frac{|\omega|}{g(\omega)}\hat{z} - l_0 \tag{37}$$

$$l_0 = -\frac{1}{J}(k_2\phi_2|e_2|^{\phi_2-1}) \tag{38}$$

with the adaptive laws

$$\dot{\hat{\mu}} = \frac{1}{J}s(k_2\phi_2|e_2|^{\phi_2-1}\eta_2(\hat{z}(\sigma_0 - \sigma_1 \frac{|\omega|}{g(\omega)}) + \sigma_1\omega)) \tag{39}$$

$$\dot{\hat{v}} = \frac{1}{J}s(k_2\phi_2|e_2|^{\phi_2-1})\sigma_2\omega\eta_3 \tag{40}$$

$$\dot{\hat{\Delta}} = \frac{1}{J}(k_2\phi_2|e_2|^{\phi_2-1})\eta_1 \tag{41}$$

there exist parameter  $\mu > 0, v > 0, \eta_1 > 0, \eta_2 > 0, \eta_3 > 0$ , then the tracking error of the closed-loop system (35) converges to zero within finite time.

*Proof:* Consider the closed-loop system (35). The Lyapunov function candidate as

$$V = \frac{1}{2}s^2 + \frac{1}{2}\mu\tilde{z}^2 + \frac{1}{2\eta_1}\tilde{\Delta}^2 + \frac{1}{2\eta_2}\tilde{\mu}^2 + \frac{1}{2\eta_3}\tilde{v}^2 \tag{42}$$

The time derivative of (42) is expressed as follows:

$$\begin{aligned}
 \dot{V} = & s\dot{s} + \mu\tilde{z}\dot{\tilde{z}} + \frac{1}{\eta_1}\tilde{\Delta}\dot{\tilde{\Delta}} + \frac{1}{\eta_2}\tilde{\mu}\dot{\tilde{\mu}} + \frac{1}{\eta_3}\tilde{v}\dot{\tilde{v}} \\
 = & -k_2k_3\phi_2|e_2|^{\phi_2-1}|s| - k_2k_4\phi_2|e_2|^{\phi_2-1}s^2 \\
 & + \frac{1}{J}sk_2\phi_2|e_2|^{\phi_2-1}(\mu z - \hat{\mu}\hat{z})(\sigma_0 - \sigma_1 \frac{|\omega|}{g(\omega)}) \\
 & + \frac{\omega}{J}s(k_2\phi_2|e_2|^{\phi_2-1})(\tilde{\mu}\sigma_1 + \tilde{v}\sigma_2) \\
 & + \frac{1}{J}s(k_2\phi_2|e_2|^{\phi_2-1})\tilde{\Delta} + \mu\tilde{z}\dot{\tilde{z}} \\
 & - \frac{1}{\eta_1}\tilde{\Delta}\dot{\tilde{\Delta}} - \frac{1}{\eta_2}\tilde{\mu}\dot{\tilde{\mu}} - \frac{1}{\eta_3}\tilde{v}\dot{\tilde{v}} \tag{43}
 \end{aligned}$$

where  $\tilde{\Delta} = \Delta - \hat{\Delta}, \tilde{\mu} = \mu - \hat{\mu}, \tilde{v} = v - \hat{v}, \tilde{z} = z - \hat{z}, \mu z - \hat{\mu}\hat{z} = \mu\tilde{z} + \tilde{\mu}\hat{z}$  Then the equation (43) can be rewritten as follows

$$\begin{aligned}
 \dot{V} = & -k_2k_3\phi_2|e_2|^{\phi_2-1}|s| - k_2k_4\phi_2|e_2|^{\phi_2-1}s^2 - \frac{\sigma_0|\omega|}{g(\omega)}\mu\tilde{z}^2 \\
 & + \tilde{\mu}(\frac{1}{J}k_2\phi_2|e_2|^{\phi_2-1}s\hat{z}(\sigma_0 - \sigma_1 \frac{|\omega|}{g(\omega)})) \\
 & + \frac{1}{J}k_2\phi_2|e_2|^{\phi_2-1}s\omega\sigma_1 - \frac{1}{\eta_2}\dot{\tilde{\mu}} \\
 & + \tilde{v}(\frac{1}{J}k_2\phi_2|e_2|^{\phi_2-1}s\omega - \frac{1}{\eta_3}\dot{\tilde{v}})
 \end{aligned}$$

$$\begin{aligned}
 & + \mu\tilde{z}(\frac{1}{J}k_2\phi_2|e_2|^{\phi_2-1} + l_0) \\
 & + \tilde{\Delta}(\frac{1}{J}k_2\phi_2|e_2|^{\phi_2-1} - \frac{1}{\eta_1}\dot{\tilde{\Delta}}) \tag{44}
 \end{aligned}$$

Substituting equation (36)-(41) into equation (44), it follows that

$$\dot{V} \leq -k_2k_3\phi_2|e_2|^{\phi_2-1}|s| - k_2k_4\phi_2|e_2|^{\phi_2-1}s^2 - \frac{\sigma_0|\omega|}{g(\omega)}\mu\tilde{z}^2 \tag{45}$$

where the function  $g(\omega)$  is positive and known. And  $\sigma_0 > 0, 1 < \phi_2 < 2, k_2 > 0, k_3 > 0, k_4 > 0$  and  $\mu > 0$ . Thus, the term  $-k_2k_3\phi_2|e_2|^{\phi_2-1}|s| \leq 0$ , the term  $-k_2k_4\phi_2|e_2|^{\phi_2-1}s^2 \leq 0$  and  $-\frac{\sigma_0|\omega|}{g(\omega)}\mu\tilde{z}^2 \leq 0$ . Then

$$\dot{V} \leq 0 \tag{46}$$

holds.

Therefore, according to the Lyapunov stability theory, the the closed-loop system (35) is asymptotical convergence. Furthermore, to showcase this convergence occurs in finite time, equation (45) can be can be rewritten as (47)

$$\begin{aligned}
 \dot{V} = & \frac{dV}{dt} \leq -k_2k_3\phi_2|e_2|^{\phi_2-1}|s| - k_2k_4\phi_2|e_2|^{\phi_2-1}s^2 \\
 & - \frac{\sigma_0|\omega|}{g(\omega)}\mu\tilde{z}^2 \\
 \leq & -k_2k_3\phi_2|e_2|^{\phi_2-1}|s| - k_2k_4\phi_2|e_2|^{\phi_2-1}s^2 \\
 = & -\rho_1(e_2)V_s^{1/2} - \rho_2(e_2)V_s^{1/2} \tag{47}
 \end{aligned}$$

where  $\rho_1(e_2) = \sqrt{2}k_2k_3\phi_2|e_2|^{\phi_2-1}, \rho_2(e_2) = 2k_2k_4\phi_2|e_2|^{\phi_2-1}$  and  $V_s = \frac{1}{2}s^2 > 0$ . By virtue of Lemma 1 and inequality (47), the tracking error (35) converges to the zero in finite time and the reaching time  $T_r$  is presented as follows:

$$T_r \leq \frac{2}{\rho_1} \ln(\frac{\rho_1 V(0)^{1/2} + \rho_2}{\rho_2}) \tag{48}$$

where  $V_s(0)$  is the initial value of  $V_s(t)$ . This completes the proof. ■

*Remark 3:* No matter where trajectories of the electro-optical targeting system (6) are, the proposed sliding mode surface  $s(t)$  is able to converge to zero within finite time. In addition, based on Lemma 2, accompanied by error trajectories of the electro-optical targeting system (6) move towards to zero, the sliding mode manifold  $s(t)$  reaches to zero within finite time. Then sliding mode time  $T_s$  is obtained is

$$\begin{aligned}
 T_s = & \int_0^{e_1(t_0)} \frac{k_2^{1/\phi_2}}{(e_1(t) + k_1 e_1(t)^{\phi_1})^{1/\phi_2}} dx \\
 = & \frac{\phi_2|e_1(t_0)|^{1-1/\phi_2}}{k_1(\phi_2 - 1)} \\
 & \cdot F(\frac{1}{\phi_2}, \frac{\phi_2 - 1}{(\phi_1 - 1)\phi_2}; 1 + \frac{\phi_2 - 1}{(\phi_1 - 1)\phi_2}; -k_1|e_1(t_0)|^{\phi_1-1}) \tag{49}
 \end{aligned}$$

where  $e_1(t_0)$  is the initial value of  $e_1(t)$ .

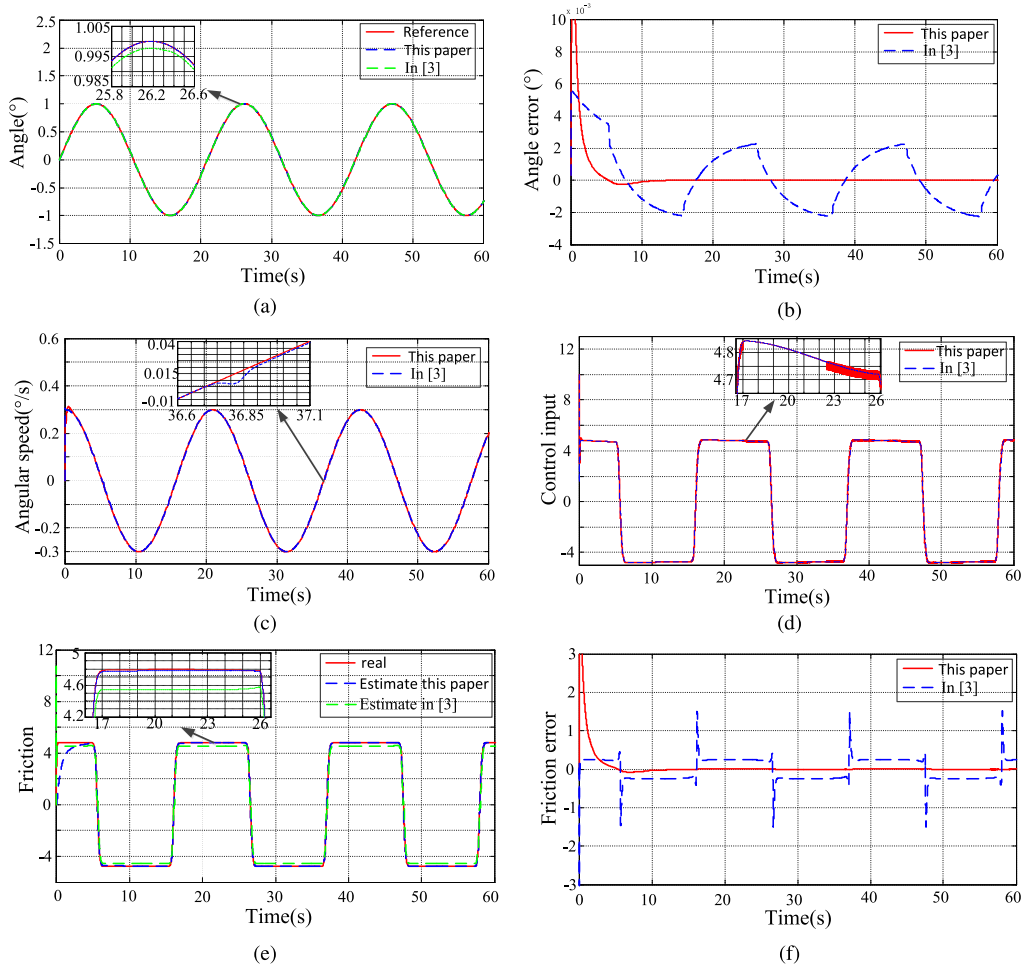


FIGURE 3. sinusoidal trajectory tracking simulation.

Remark 4: The main characteristics of the proposed robust adaptive NFTSM are as follows: (a) The response rapidity performance can be speed up owing to the fast finite-time convergence. The parameters  $k_1, k_2, \phi_1$  can be adjusted based on Equation(49) to change the convergence time; (b) The characteristics of strong robustness of NFTSM properties make it possible to overcome disturbance torque and nonlinear friction. (c) Owing to the absence of negative power term in control law Equation(37),the singularity problem can be avoided.

IV. SYSTEM SIMULATION

Simulation is done in this section to validate the effectiveness of designed control strategy before practical experiments. In addition, the proposed control strategy has been compared with the method in [3], in which an AIBSM controller was introduced for electro-optical targeting system. The parameters of the electro-optical targeting system is shown in Table 1. The sinusoidal angle reference signal is  $1^\circ$  with  $0.3Hz$ . The simulation results within  $60s$  are depicted in Fig.3. Fig.3(a) demonstrates that the tracking angle in this paper almost coincident with the reference signal. Fig.3(b) depicts

TABLE 1. System parameters.

Parameters	Value
Inertia( $kgm^2$ )	$J = 1.32$
Stiction force(Nm)	$F_s = 1.52$
Coulomb friction(Nm)	$F_c = 4.78$
Stiffness coefficient(Nm/deg)	$\sigma_0 = 473$
Damping coefficient(Nms/deg)	$\sigma_1 = 0.87$
Viscous friction coefficient(Nms/deg)	$\sigma_2 = 0.0025$
Stribeck angle velocity(deg/s)	$\omega_s = 0.01$
Torque coefficient(Nm/A)	$K_t = 4.65$
Back-EMF coefficient(Vs/deg)	$K_e = 0.1$
Motor resistance( $\Omega$ )	$R = 4.62$

that the angle tracking error proposed in this paper is less than in [3]. Fig.3(c) illustrates that the angle speed curve. It can be seen that the "dead zone" is nearly eliminated by proposed control approach whenever angle speed goes through zero. The controllers, friction, friction observation and their comparative results with [3] are displayed in Fig.3(d)(e)(f). Obviously, the friction observe in this paper achieves a better estimation of friction than in [3]. It is well evident that the proposed control strategy has enough capability to track the reference angle in theory. And the proposed control strategy is suitable for electro-optical targeting system.

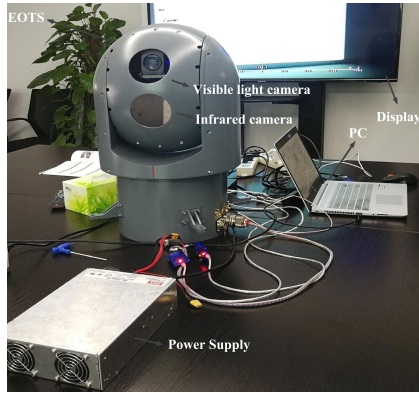


FIGURE 4. The electro-optical targeting system.

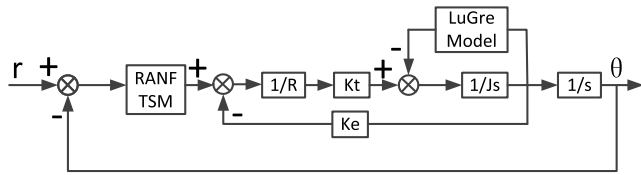


FIGURE 5. Structure diagram of electro-optical targeting system.

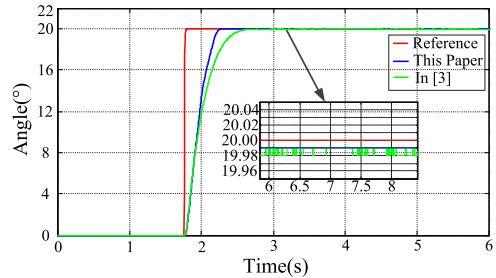
V. EXPERIMENTS AND RESULTS

Experiments are conducted and the experiment results are presented in this section to fully prove the validity and practicability of the finite-time robust adaptive nonsingular fast terminal sliding mode control strategy. A single gimbal of electro-optical targeting system in axis of azimuth is studied, which is shown in Fig.4. The structure diagram of electro-optical targeting system is presented in Fig.5. The experimental platform contains five main parts: DSP, permanent magnet DC motor, absolute magnetic rotary encoder, motor driver and payload with visible light camera and infrared camera. The absolute magnetic rotary encoder with 0.01° resolution are utilized for angle measurement on each axis. Note that in the following experiments, the commands from PC are regarded as the reference angle trajectory tracking signals.

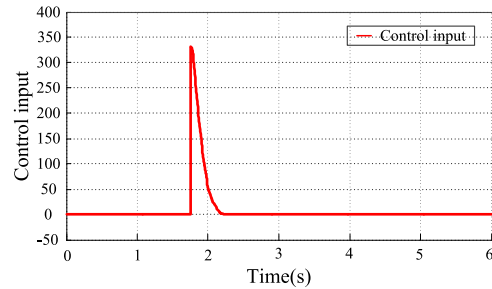
A. STEP EXPERIMENT

In the first angle trajectory tracking experiment, a step signal with 20° within 6s based on finite-time robust adaptive sliding mode control strategy is shown in Fig.6(a) in blue curve. It is apparent that the angle  $y$  tracks the reference input  $y_r$  quickly and accurately without any overshoot. Furthermore, the gimbal of electro-optical targeting system in axis of azimuth reaches the set angle in about 0.9s and the steady-state error is about 0.01°. The control input signal of the electro-optical targeting system is the digital signal from DSP. The trend of digital control signal is presented in Fig.6(b), besides, it reduces to zero after about 0.9s. At this state, the gimbal is at the angle of 20°. The angle tracking error is depicted in Fig.6(c). It is obviously that the angle error in steady state is about 0.01°, which is nearly about 0.05% of the total angle of travel.

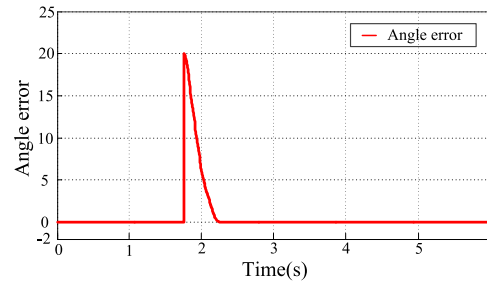
The comparing experimental results for tracking a step signal is also shown in Fig.6(a). The step response in green curve is based on the control strategy proposed in [3].



(a)



(b)



(c)

FIGURE 6. Step trajectory tracking experiment.

The convergence rate by proposed control strategy is faster than that in [3]. In addition, the closed-loop system based on proposed control strategy has better vibration characteristics. The oscillations of green curve in Fig.6(a) in steady state is obvious, while the blue curve tracks the desired input  $r$  without any oscillations. Therefore, it is concluded that the finite-time robust adaptive sliding mode control strategy for electro-optical targeting system is effective.

B. SINUSOIDAL SIGNAL EXPERIMENT

In the second angle trajectory tracking experiment, a sinusoidal signal with frequency 0.01Hz and amplitude 20° during 60s is given as a desired angle tracking trajectory for the gimbal of electro-optical targeting system in axis of azimuth. The experimental result is shown in Fig.7. Obviously, angle  $y$  tracks the given reference signal  $y_r$  smoothly with very small phase difference shown in Fig.7(a). In comparing tracking experiment based on [3] shown in Fig.7(b), the angle  $y$  tracks the given reference signal  $y_r$  smoothly with larger error and phase difference. Fig.7(c) displays the digital control input. Note that the curve of control input is different from the simulation in Fig.3(e). Because in Fig.3(e) the desired tracking angle 1° is very small compared to the desired tracking



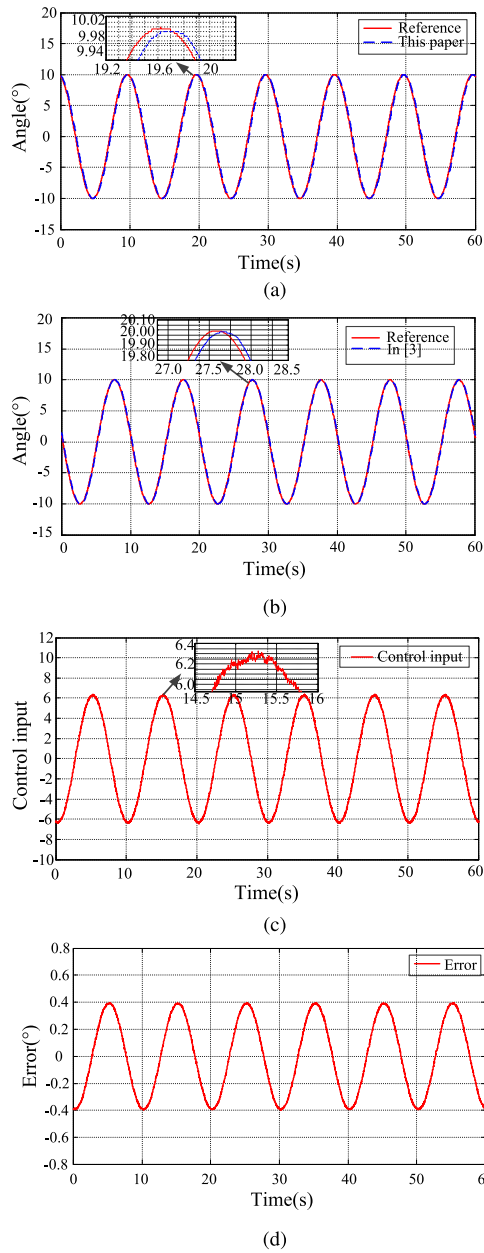


FIGURE 7. Sinusoidal trajectory tracking experiment.

angle  $10^\circ$  in practical experiment, in simulation the control input contributes the most to deal with friction whereas in practical experiment the control input corresponds to track desired angle. The tracking error is shown in Fig.7(d) and it can be seen that the maximum peak-to-peak error is about  $0.78^\circ$  which accounts for about 3.9% of the total angle amplitude. In addition, the error result in this paper is much smaller than that the control strategy in [3] which is about  $1.32^\circ$  accounting about 6.6% of the total angle amplitude. To quantify the angle tracking behaviors of the controller, the root mean square (RMS) is analyzed. The rms tracking error of the controller in this paper reaches about 0.2789 while the controller based on [3] is about 0.4240. The comparison data is shown in table 2. Thus, it is well evident that the finite-time

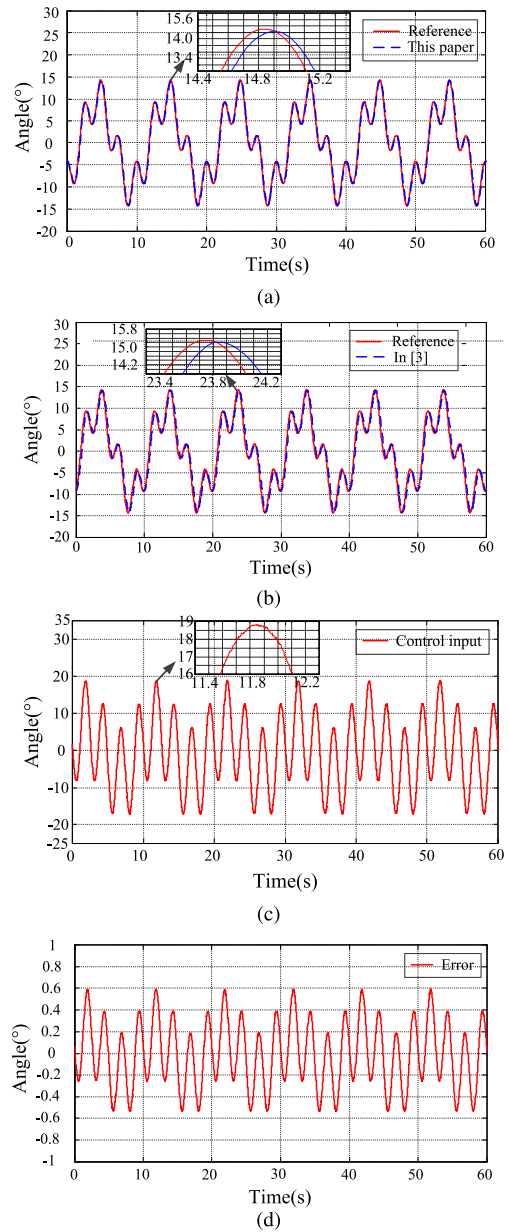


FIGURE 8. Multiple sinusoidal trajectory tracking experiment.

TABLE 2. Comparison data in experiment B.

controller	This paper	In [3]
MAX	$0.78^\circ$	$1.32^\circ$
Percentage	3.9%	6.6%
RMS	0.2789	0.4240

robust adaptive sliding mode control strategy is precisely and smoothly with little time-delays in the application of sinusoidal angle trajectory tracking with low frequency.

### C. MULTIPLE SINUSOIDAL SIGNAL EXPERIMENT

In the third angle trajectory tracking experiment, a multiple sinusoidal signal with frequency 0.01Hz, amplitude  $20^\circ$  and frequency 0.04Hz, amplitude  $10^\circ$  within 60s is given as a desired angle tracking trajectory for the gimbal of

electro-optical targeting system in axis of azimuth. The experimental results are shown in Fig.8. It can be seen that the control strategy designed in this paper outperforms the method in [3], realizes capturing the given reference signal  $y_r$  smoothly with little error and phase difference as shown in Fig.8(a) and Fig.8(b), Fig.8(c) depicts the digital control input. The tracking error behavior in term of time is shown in Fig.8(d). The maximum peak-to-peak error is less than  $1.13^\circ$  which accounts for about 3.9% of the maximum angle amplitude. Meanwhile, the maximum peak-to-peak error in [3] is  $2.76^\circ$  which accounts for about 9.2% of the maximum angle amplitude. The root mean square (RMS) is analyzed. The rms tracking error of proposed controller in this paper approaches about 0.3081 while the controller based on [3] reaches about 0.7002. The comparison data is shown in table 3.

**TABLE 3. Comparison data in experiment C.**

controller	This paper	In [3]
MAX	1.13 °	2.76 °
Percentage	3.9%	9.2%
RMS	0.3081	0.7002

The above three experimental results validate that the finite-time robust adaptive sliding mode control strategy designed in this paper has good capability to track the angle with different frequency. And it is superior to the method in [3]. Therefore, it is concluded that this control strategy is capable of achieving high accuracy, fast response and good stability performance being confronted with nonlinear friction as well as disturbance torque.

## VI. CONCLUSION

In this paper, accurate angle control was investigated for electro-optical targeting system via a novel finite-time robust adaptive nonsingular fast terminal sliding mode control strategy. The proposed control strategy integrates the advantages of robust adaptive control and NFTSM control. The robust adaptive control with friction observation was applied to estimate nonlinear friction and disturbance torque. Meanwhile, a NFTSM control are integrated into the robust adaptive control approach to guarantee response rapidity and strengthen the robustness. Furthermore, the closed-loop system is proved by Lyapunov methods within finite time. Finally, simulation and real experiment results validate the control strategy.

Future work intends to concentrate on a second-order sliding mode (SOSM) control algorithm [36] and disturbance observer [37] to address disturbance torque and nonlinear friction. And experimental verification on electro-optical targeting system.

## REFERENCES

- [1] B. Guan, J. Jia, Y. Zhu, and C. Lei, "The strategy of three-axis photoelectric tracking system without blind region," *Mech. Mach. Theory*, vol. 56, pp. 89–98, Oct. 2012.
- [2] J.-H. Kim, D. W. Lee, K.-R. Cho, S.-Y. Jo, J.-H. Kim, C.-O. Mim, D.-I. Han, and S.-J. Cho, "Development of an electro-optical system for small UAV," *Aerosp. Sci. Technol.*, vol. 14, pp. 505–511, Oct./Nov. 2010.
- [3] F. Yue, X. Li, C. Chen, and W. Tan, "Adaptive integral backstepping sliding mode control for opto-electronic tracking system based on modified LuGre friction model," *Int. J. Syst. Sci.*, vol. 48, pp. 3374–3381, Nov. 2017.
- [4] D. Naso, F. Cupertino, and B. Turchiano, "Precise position control of tubular linear motors with neural networks and composite learning," *Control Eng. Pract.*, vol. 18, no. 5, pp. 515–522, May 2010.
- [5] L. Qing, Z. Jian, and W. Yang, "Adaptive backstepping friction compensation control based on modified LuGre model," *Small Special Electr. Mach.*, vol. 39, pp. 67–79, Mar. 2011.
- [6] Y. Zhang, P. Yan, and Z. Zhang, "High precision tracking control of a servo gantry with dynamic friction compensation," *ISA Trans.*, vol. 62, pp. 349–436, May 2016.
- [7] J. Yao, W. Deng, and Z. Jiao, "Adaptive control of hydraulic actuators with LuGre model-based friction compensation," *IEEE Trans. Ind. Electron.*, vol. 62, no. 10, pp. 6469–6477, Oct. 2015.
- [8] F. Farhani, C. B. Regaya, A. Zaafour, and A. Chaari, "Real time PI-backstepping induction machine drive with efficiency optimization," *ISA Trans.*, vol. 70, pp. 348–356, Sep. 2017.
- [9] A. Zaafour, C. B. Regaya, H. B. Azza, and A. Chaari, "DSP-based adaptive backstepping using the tracking errors for high-performance sensorless speed control of induction motor drive," *ISA Trans.*, vol. 60, pp. 333–347, Jan. 2016.
- [10] Y. Liu, X. P. Liu, Y. W. Jing, and S. W. Zhou, "Adaptive backstepping  $H_\infty$  tracking control with prescribed performance for Internet congestion," *ISA Trans.*, vol. 72, pp. 92–99, Jan. 2018.
- [11] W. Deng and J. Yao, "Adaptive integral robust control and application to electromechanical servo systems," *ISA Trans.*, vol. 67, pp. 256–265, Mar. 2017.
- [12] J. Wu and Y. Lu, "Adaptive backstepping sliding mode control for boost converter with constant power load," *IEEE Access*, vol. 7, pp. 50797–50807, 2019.
- [13] Z. Tian, J. Yuan, L. Xu, X. Zhang, and J. Wang, "Model-based adaptive sliding mode control of the subcritical boiler-turbine system with uncertainties," *ISA Trans.*, vol. 79, pp. 161–171, Aug. 2018.
- [14] W. Guo and D. Liu, "Sliding mode observe and control for the underactuated inertia wheel pendulum system," *IEEE Access*, vol. 7, pp. 86394–86402, 2019.
- [15] Z. Song, K. Sun, and S. Ling, "Stabilization and synchronization for a mechanical system via adaptive sliding mode control," *ISA Trans.*, vol. 68, pp. 353–366, May 2017.
- [16] A. Ayadi, M. Smaoui, S. Aloui, S. Hajji, and M. Farza, "Adaptive sliding mode control with moving surface: Experimental validation for electropneumatic system," *Mech. Syst. Signal Process.*, vol. 109, pp. 27–44, Sep. 2018.
- [17] S. Baek, J. Baek, and S. Han, "An adaptive sliding mode control with effective switching gain tuning near the sliding surface," *IEEE Access*, vol. 7, pp. 15563–15572, 2019.
- [18] M. Chen, Q.-X. Wu, and R.-X. Cui, "Terminal sliding mode tracking control for a class of SISO uncertain nonlinear systems," *ISA Trans.*, vol. 52, pp. 198–206, Mar. 2013.
- [19] L. Wang, T. Chai, and L. Zhai, "Neural-network-based terminal sliding-mode control of robotic manipulators including actuator dynamics," *IEEE Trans. Ind. Electron.*, vol. 56, no. 9, pp. 3296–3304, Sep. 2009.
- [20] S.-Y. Chen and F.-J. Lin, "Robust nonsingular terminal sliding-mode control for nonlinear magnetic bearing system," *IEEE Trans. Control Syst. Technol.*, vol. 19, no. 3, pp. 636–643, May 2011.
- [21] Y. Feng, X. Yu, and Z. Man, "Non-singular terminal sliding mode control of rigid manipulators," *Automatica*, vol. 38, no. 12, pp. 2159–2167, Dec. 2002.
- [22] X. Yu, Z. Man, Y. Feng, and Z. Guan, "Nonsingular terminal sliding mode control of a class of nonlinear dynamical systems," *IFAC Proc. Volumes*, vol. 35, no. 1, pp. 161–165, 2002.
- [23] S. S.-D. Xu, C.-C. Chen, and Z.-L. Wu, "Study of nonsingular fast terminal sliding-mode fault-tolerant control," *IEEE Trans. Ind. Electron.*, vol. 38, no. 62, pp. 3906–3913, Jun. 2015.
- [24] M. L. Corradini and A. Cristofaro, "Nonsingular terminal sliding-mode control of nonlinear planar systems with global fixed-time stability guarantees," *Automatica*, vol. 95, pp. 561–565, Sep. 2018.
- [25] C. Xiu and P. Guo, "Global terminal sliding mode control with the quick reaching law and its application," *IEEE Access*, vol. 6, pp. 49793–49800, 2018.

- [26] A. Safa, R. Y. Abdolmalaki, S. Shafiee, and B. Sadeghi, "Adaptive nonsingular terminal sliding mode controller for micro/nanopositioning systems driven by linear piezoelectric ceramic motors," *ISA Trans.*, vol. 77, pp. 122–132, Jun. 2018.
- [27] J. Fang and R. Yin, "An adaptive nonlinear control for gyro stabilized platform based on neural networks and disturbance observer," *Math. Problems Eng.*, vol. 2014, Nov. 2014, Art. no. 472815.
- [28] V. Lampaert, J. Swevers, and F. Al-Bender, "Modification of the Leuven integrated friction model structure," *IEEE Trans. Autom. Control.*, vol. 47, no. 4, pp. 683–687, Apr. 2002.
- [29] P. Dupont, V. Hayward, B. Armstrong, and F. Altpeter, "Single state elastoplastic friction models," *IEEE Trans. Autom. Control.*, vol. 47, no. 5, pp. 787–792, May 2002.
- [30] C. C. de Wit, H. Olsson, K. J. Åström, and P. Lischinsky, "A new model for control of systems with friction," *IEEE Trans. Autom. Control.*, vol. 40, no. 3, pp. 419–425, Mar. 1995.
- [31] X. Wang and S. Wang, "High performance adaptive control of mechanical servo system with LuGre friction model: Identification and compensation," *J. Dyn. Syst., Meas., Control.*, vol. 134, Jan. 2012, Art. no. 011021.
- [32] Y. Yang, C. Hua, and X. Guan, "Adaptive fuzzy finite-time coordination control for networked nonlinear bilateral teleoperation system," *IEEE Trans. Fuzzy Syst.*, vol. 22, no. 3, pp. 631–641, Jun. 2014.
- [33] L. Yang and J. Yang, "Nonsingular fast terminal sliding-mode control for nonlinear dynamical systems," *Int. J. Robust Nonlinear Control.*, vol. 21, no. 16, pp. 1865–1879, Nov. 2011.
- [34] M. Abramowitz and I. A. Stegun, *Handbook of Mathematical Functions: With Formulas, Graphs, and Mathematical Tables*. New York, NY, USA: Dover, 1972.
- [35] S. Ding, K. Mei, and S. Li, "A new second-order sliding mode and its application to nonlinear constrained systems," *IEEE Trans. Autom. Control.*, vol. 64, no. 6, pp. 2545–2552, Jun. 2019.
- [36] S. Ding, W. Chen, K. Mei, and D. J. Murray-Smith, "Disturbance observer design for nonlinear systems represented by input–output models," to be published.
- [37] S. Ding, W. Chen, K. Mei, and D. J. Murray-Smith, "Disturbance observer design for nonlinear systems represented by input–output models," *IEEE Trans. Ind. Electron.*, vol. 67, no. 2, pp. 1222–1232, Feb. 2020.



**XINLI ZHOU** received the B.S. degree in automation from the Wuhan University of Science and Technology, Hubei, China, in 2015, and the M.S. degree in instrumentation science and technology from Tianjin University, Tianjin, China, in 2017, where he is currently pursuing the Ph.D. degree in instrumentation science and technology.

His current research interests include robust control, active disturbance rejection control, electro-optical targeting systems, and fast-steering mirror systems.



**XINGFEI LI** received the M.S. degree in instrument science and technology from Southeast University and the Ph.D. degree from the College of Precision Instruments and Opto-Electronics Engineering, Tianjin University, Tianjin, China, in 1994 and 2000, respectively.

He worked as a Researcher with The Hong Kong Polytechnic University, Hong Kong, China, from 1996 to 1999, and did his postdoctoral research in mechanical engineering at The University of Michigan, Ann Arbor, MI, USA, from 2003 to 2004. He is currently a Professor with the College of Precision Instruments and Opto-Electronics Engineering, Tianjin University. His research interests include nonlinear control, robust control, electro-optical targeting systems, signal processing, as well as manufacture and integration of inertial sensors.

• • •